Ice Jam Modelling and Field Data Collection for Flood Forecasting in the Saint John River, New Brunswick

SPYROS BELTAOS[1], PATRICK TANG[2], AND ROBERT ROWSELL[1]

ABSTRACT

Ice jams cause major flooding and severe damages to communities and infrastructure along the Saint John River. There is a growing need to develop capability in forecasting and analyzing ice-jam-related flood events. This capability is also essential in anticipating the potential for increased ice jam damages as a result of a changing climate. The HEC-RAS model, which can simulate ice jam configuration under steady-state conditions, has been calibrated for operational application along the international Saint John River from Dickey, Maine, USA, to Grand Falls, New Brunswick, Canada. Examples of model results are presented and the modelling experience gained to date is outlined. A potentially damaging consequence of jamming is the sharp wave that is generated upon ice-jam release. Such waves, called javes for short, propagate very rapidly and can greatly amplify flow velocity and hydrodynamic forces relative to runoff waves. As modelling capability is limited for such dynamic phenomena, a field data collection program was initiated in 2007 to measure jave characteristics during the spring breakup of the ice cover. This program involves deployment of portable pressure loggers at key locations along the river. Data recording can extend well beyond the breakup event to also capture the open-water, spring flood. Representative data are presented and jave properties are compared to those of post-breakup runoff waves. Future work towards improving modelling capability is discussed.

Keywords: breakup, calibration, dynamic processes field measurements, flood forecasting, ice jam, jave, numerical modelling.

INTRODUCTION

The province of New Brunswick is home to many scenic, ecologically rich streams and most New Brunswickers live next to their banks. Along with the benefits of riverside residence, however, come flood risks. Flooding may be caused by high water volumes under open water conditions or by a combination of moderate flows and ice jams that form during breakup events. The Saint John River is the largest in the province, and prone to flooding, especially in middle and upper reaches, respectively defined as Mactaquac to Grand Falls and above Grand Falls. Ice-jam flooding in the Saint John River basin is responsible for 70% of total flood damage in the province (Humes and Dublin, 1988) and there is evidence of increasing, climate-related, severity (Hare *et al*., 1997a, 1997b; Beltaos, 2002, 2004).

To ensure the safety of the many communities and help mitigate flood impacts, the NB Hydrology Centre, which is a part of the NB Dept. of the Environment (NBENV), generates

[1] National Water Research Institute, Environment Canada, Burlington, Canada.
[2] New Brunswick Department of the Environment, Fredericton, Canada (retired).

timely flow forecasts during high runoff periods. The forecasts are based on the numerical SSARR (Streamflow Synthesis And Reservoir Regulation) model which is an open-water hydrologic model. During periods of ice effects on stage, the model cannot provide accurate water levels, but the forecasts are supplemented by frequent local observers' reports on ice conditions. Such reports help the forecasters make qualitative judgments as to immediate risks.

Ice jam prediction is a problem of major practical significance, but so far only partially solved by river ice researchers and engineers. It is not yet possible to predict whether and when an ice jam will form at a particular location and when it might release. However, modelling capability does exist for predicting the water levels caused by an ice jam given its location and extent as well as channel bathymetry and flow discharge (Beltaos, 2008). Though limited in scope, this type of modelling can be very useful in flood forecasting, especially where it can be coupled with insitu reports from local observers. To realize this potential, a modelling program was initiated, aiming at implementation, calibration, and eventual operational application of an ice-jam model on the upper Saint John River (Tang and Beltaos, 2008). This task is greatly facilitated by data collected under the Saint John River Ice and Sedimentation (SJRIS) study, which was jointly carried out in the 1990s by then NB Dept. of the Environment and Local Government (NBELG), NB Power and the National Water Research Institute (NWRI) of Environment Canada.

A secondary, but also potentially damaging, consequence of jamming is the sharp wave that is generated upon ice-jam release. Such waves, called "javes" for short (Jasek and Beltaos, 2008), propagate very rapidly and can greatly amplify flow velocity and hydrodynamic forces relative to runoff waves. Such conditions can imperil people, homes, and infrastructure, and have the potential to degrade aquatic habitat via stream bank and bed erosion. As modelling capability is limited for such dynamic phenomena, a field data collection program was initiated in 2007 to measure jave characteristics during the spring breakup of the ice cover. A by-product was the collection of similar data on ordinary runoff waves caused by the spring flood under open-water flow conditions.

The objective of this paper is to report and assess the results of the modelling and field data collection activities. Following brief descriptions of the study reach and the ice regime of the upper Saint John, the choice and calibration of the ice-jam model are discussed, including an outline of problems that were encountered and adopted practical remedies. Next, the equipment and methodology used to record dynamic phenomena such as javes and runoff waves are described, followed by illustrations of typical results and wave characteristics. In the following two sections, the hydrodynamic properties of these wave types are assessed and compared. The modelling and monitoring results as well as future studies are discussed next.

STUDY REACH AND ICE REGIME OF THE UPPER ST. JOHN RIVER

The Saint John River basin (55,100 km^2) forms a broad arc across southeastern Quebec, northern Maine (USA), and western New Brunswick. The basin of the upper Saint John has a modified continental climate that is characterized by cold winters, cool summers, and no dry season. Mean annual precipitation is about 1100 mm, of which about 340 mm is snowfall. The Saint John River flows for approximately 700 km from Little Saint John Lake in the State of Maine, U.S.A. to the Bay of Fundy at Saint John, New Brunswick, Canada. The total fall of the river is about 480 m. Figure 1 is a plan view of the St. John River from Dickey (Maine) to Grand Falls (NB), site of a hydropower generating station.

From Dickey to Grand Falls, the river length is approximately 145 km. Between Dickey and Edmundston the river is steep (slope in the neighbourhood of 0.5 m/km) and has a series of rapids that can delay, or even prevent, formation of a stable local ice cover. Generally, the river from Dickey to Edmundston is relatively shallow with occasional islands. It progressively deepens in the regulated reach below Edmundston, where a few large islands are also present. Backwater caused by the Grand Falls Control Structure (GFCS) creates a relatively flat water surface that extends up to 50 km upstream depending on the prevailing river flow and GFCS operating mode.

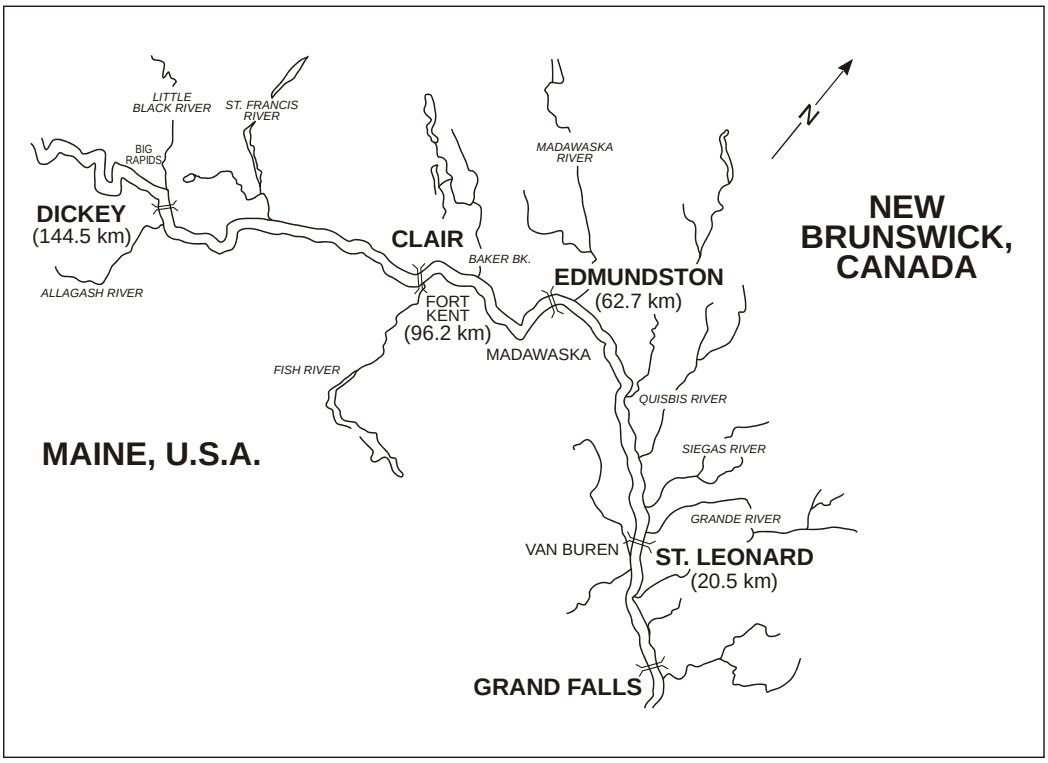

Figure 1. Planview of upper Saint John River between Dickey, Maine and Grand Falls, New Brunswick. Channel width has been exaggerated for clarity and is not to scale. Bridge locations are indicated in river kilometres above the Grand Falls Control Structure.

There are four water level recording stations in the study reach, located near Dickey, Clair/Fort Kent, Edmundston, and St. Leonard. The first two are operated by USGS (United States Geological Survey) and also provide daily discharge; data can be obtained at http://nwis.waterdata.usgs.gov/nwis/uv/?site_no=01010500&agency_cd=USGS; accessed March 16, 2011). The Edmundston station is operated by WSC (Water Survey of Canada); data can be obtained at http://www.wsc.ec.gc.ca/applications/H2O/HydromatD-eng.cfm (accessed March 16, 2011) but do not include flow after 1979. A water level gauge is operated at St. Leonard by NB Power, and these data are shared with NB Environment, one of the collaborating agencies for this study.

The remainder of this section presents a brief description of the ice regime, based on more detailed information contained in Beltaos *et al*. (2003). The ice cover normally forms between late November and late January, and most frequently in December. The first ice cover appears in the Grand Falls headpond near the control structure, and quickly advances in the calm regulated reach towards Edmundston where warm effluents from local paper mills suppress local ice formation throughout the winter. At the same time, increasing amounts of slush are generated in the more rapid, upper reaches and the resulting ice pans eventually lodge at a few key locations. Ice covers then propagate upstream from these sites. It is thus common to encounter alternating open-water and ice-covered segments in the study reach during the freeze-up period. The spatial variation of ice thickness reflects differences in freeze-up timing and rate of freezing. Generally, the thickest ice is encountered near Dickey and Grand Falls. The Clair-Fort Kent reach freezes last and has the thinnest cover, typically attaining 0.5 m by the end of the winter.

Generally, spring breakup events occur in April and follow a common pattern. As temperatures rise and approach 0°C, the ice cover downstream of Edmundston begins to recede in the

downstream direction, owing to enhanced heat transfer at the open-water surface. When significant runoff is under way, the ice cover on several river sections between Clair and Dickey begins to break up, and small jams may form. With increasing flows, these jams eventually dislodge to form one or two major jams upstream of Clair. By this time, the relatively thin ice cover at and below Clair has already moved out and formed a short jam near Baker Brook (Fig. 1). When the above-Clair jams release, major ice runs occur that may be arrested and cause flooding at Baker Brook. More commonly, however, the ice runs easily dislodge the remaining sheet ice cover as far as Edmundston, and advance unhindered until they encounter the receding edge of the sheet-ice cover downstream of Edmundston. In this area, the relative thickness and strength of the local ice cover and the low slope of the water surface can produce major ice jams and floods (e.g. 1991, 1993, near Ste-Anne de Madawaska, indicated simply as "Ste-Anne" on map). On occasion, breakup may also occur in the winter as a result of a brief thaw and rainfall. Such events do not follow the above pattern and are often incomplete by the time the cold weather resumes (Beltaos *et al*., 2003).

SELECTION AND FEATURES OF ICE JAM MODEL

Several public domain models of ice jams are available (e.g. ICEJAM, RIVJAM, HEC-RAS; Carson *et al*., 2011). They are based on similar differential equations (steady-state one-dimensional flow; stability of ice rubble, which is considered a granular medium); however, they utilize different solution methods and assumptions concerning the key conditions at the toe (downstream end of the jam). For operational use, the HEC-RAS model is the most convenient: once implemented, it provides a platform for computations under any type of hydraulic condition, such as open-water flow, sheet-ice cover, ice jam, and any combination of these within the study reach.

In addition to bathymetric information, the ice option of HEC-RAS (or HR for short) requires the following input:

-River discharge (Q) at the upstream end of the computational reach and at the confluences of significant tributaries.
-Boundary condition at the downstream end of the computational reach, e.g. known water level or normal flow depth.
-Any observed water levels that may be available within the computational reach, to be used in graphical illustrations of calibration runs (optional).
-Locations of toe (downstream end) and head (upstream end) of an ice jam.
-Upstream and downstream limits of open-water and sheet-ice cover reaches.
-Manning coefficients of river bed and sheet ice cover (n_b, n_i).
-Thickness of sheet ice cover (h_i).
-Manning coefficient, n_J, of the underside of an ice jam. This can be a user-specified value, applicable to the entire length of the jam, or a model-generated function of jam thickness (Nezhikhovskiy, 1964). The latter option is used exclusively herein, based on early runs that indicated improved model performance (Tang and Beltaos, 2008) as well as on extensive empirical evidence (Beltaos, 2001; Carson et al., 2011).
-Porosity (p) of the rubble comprising the jam; invariably taken as 0.40.
-Internal friction angle (φ) of the rubble comprising the jam; default value = 45°.
-Ratio of lateral-to-longitudinal stresses within the rubble mass (K_1); default value = 0.33. The user's manual offers no other guidance on how to select K_1; consequently the default value has been used in all runs described herein. Detailed information on K_1 can be found in Flato and Gerard (1986), on whose work the HR ice option is based, and in Beltaos (2010).
-Maximum allowable flow velocity underneath the jam (V_{max}); default value = 1.5 m/s. It is assumed that if this limiting value is exceeded, ice blocks within the jam will be mobilized and transported away by the flow. It is well known that ice jams are thickest near their "toe" (or downstream end), as a result of large local water surface slopes (Beltaos and Wong, 1986;

Beltaos, 2001). The resulting reduction in unobstructed flow area causes an increase in the mean under-ice velocity (V) if flow through the voids of the jam is neglected as is done in HR. Where a jam thickens to the extent that the under-ice velocity (V) exceeds V_{max}, HR ignores the stability equation and computes the jam profile by setting $V = V_{max}$. It is therefore implicitly assumed that the jam is continuously collapsing within such regions, being prevented from attaining the stability-dictated thickness because it is being eroded by the flow. The length of the jam is assumed to be maintained by the arrival of new ice to the head of the jam. On the other hand, models that do take into account flow through the voids of the jam (e.g. RIVJAM; Beltaos, 1993; 1999) can satisfy stability throughout the jam length without generating excessive V-values.

MODEL CALIBRATION

For the present study, channel bathymetry was specified by two sets of cross sections (XSs for short), respectively surveyed by NB Power in the 1920s and by the National Water Research Institute of Environment Canada in the 1990s. Several ice-jam data sets, obtained during the SJRIS study (Beltaos *et al.*, 1994; Beltaos and Burrell, unpublished data), were used to calibrate the model. From gauge data under open-water and sheet-ice cover conditions, it was determined that $n_i = 0.020$ and $n_b = 0.025$ to 0.033, depending on location (0.025 at and below km 71.0; 0.033 at and above km 83.1; gradual transition between kms 71.0 and 83.1; all km values represent river distances upstream of the GFCS).

For each ice jam data set, the following calibration procedure was adopted: (1) adjust the internal friction angle, keeping all other parameters at default values (or relationships), until good agreement with the available water level measurements is obtained; (2) if this procedure does not result in satisfactory prediction, adjust the value of V_{max} and repeat.

Figure 2 illustrates model results for a 1991 ice jam near the community of Ste-Anne using values of 1.5 m/s and 56° for V_{max} and φ; the same set of parameters also gave good results with data from major ice jams that formed near Ste-Anne in 1993 and 2009. Figure 3 illustrates the upstream extent of the backwater caused by the 2009 jam and shows good prediction of gauge-derived water levels far upstream of the jam.

In Figs. 2 and 3, the channel thalweg is the line connecting the deepest points of the surveyed XSs within the study reach and provides a visual impression of the riverbed. Of course, the average flow depth is less than what is indicated by the thalweg and water surface lines. Nevertheless, taken over extended reaches, the thalweg does indicate the general slope of the river, which (as expected) is similar to that of the water surface if there are no regulation or ice-jam influences (e.g. ~ km 70 to 95; Fig. 3). The data points on the thalweg line also serve to show where the surveyed XSs are located. In general, the spacing between successive sections does not exceed 2 km, while the very close spacing in the range 30 to 35 km is due to detailed surveys that were carried out to study toe conditions of the 1991 ice jam (Beltaos *et al*., 1996).

During the initial calibration of the model, Tang and Beltaos (2008) encountered practical difficulties that were partly resolved by using an external interpolation routine to generate new XSs between surveyed ones that were too far apart. The current version of HEC-RAS (http://www.hec.usace.army.mil/software/hec-ras/; accessed March 11, 2011) includes a convenient interpolation "tool" that generates additional XSs, as needed to ensure that the spacing between successive sections is no more than, and as close as possible to, a user-specified value ΔL.

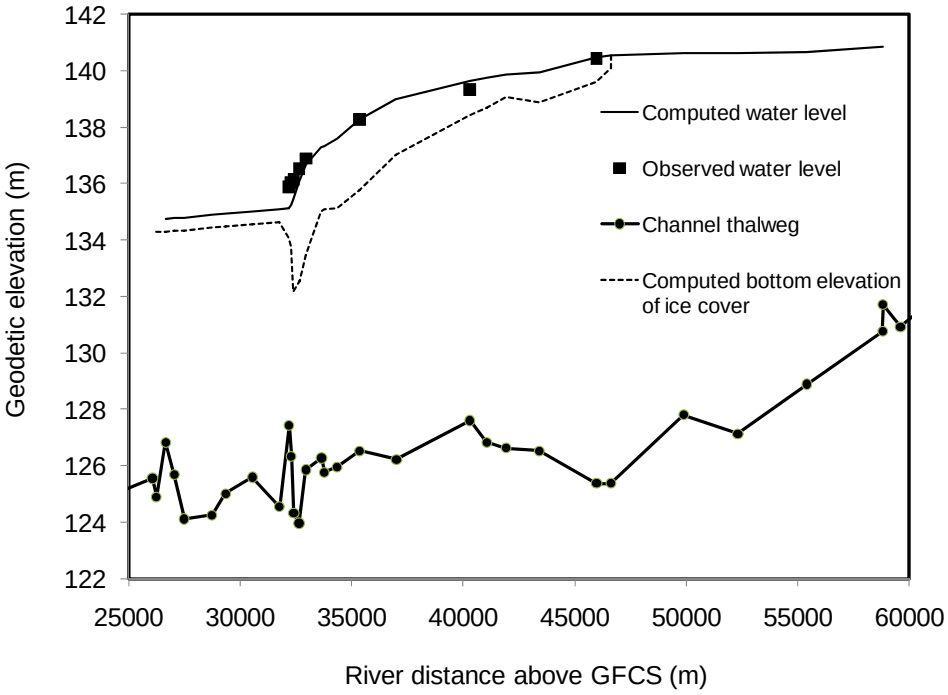

Figure 2. Model output versus measurements, ice jam near Ste-Anne, April 12, 1991.

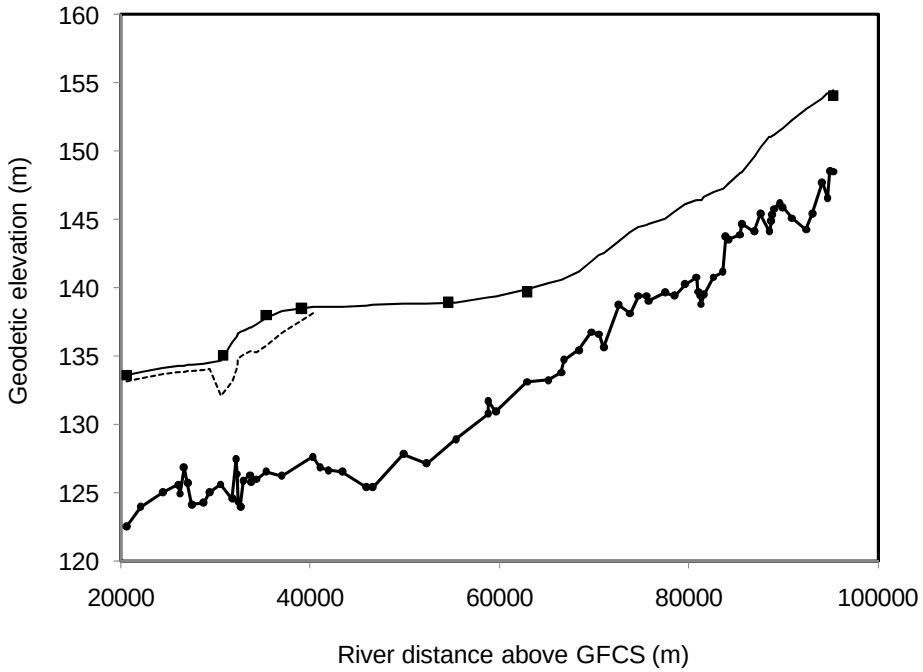

Figure 3. Model output versus measurements, April 8, 2009. Same legend as in Fig. 2. The last two data points were obtained from gauge records at Edmundston (~ 63 km) and Fort Kent (~ 95 km).

The interpolation tool was used to explore how cross-sectional spacing might affect model output in the case of the 1991 Ste-Anne ice jam, for which the channel width is about 200 m. It

was fully expected that output would improve with decreasing ΔL and remain unchanged below some threshold value of ΔL. This feature is not only common for numerical solutions, but also coincides with what was recommended for the ICEJAM model (Flato and Gerard, 1986), which formed the basis for the ice jam routine of HEC-RAS. The latter authors had reported that test runs with an assumed prismatic channel showed that solutions remained unchanged below a spacing of one-quarter of the channel width.

Contrary to expectation, it was found that the value of ΔL may have a large influence on the output of the model, while no convergence to a stable solution could be obtained. As ΔL decreased to ~ 300 m, the computed jam thickness and water surface elevations remained essentially unchanged, but changed as ΔL was reduced to 200, 100, 50 (~ ¼ of channel width), and 20 m. For the 50 m spacing, the model output is illustrated in Fig. 4, which shows considerable deterioration relative to the graph of Fig. 2. The results of these test runs are summarized in Table 1, where t_J is a representative value of the jam thickness within its intermediate reach, that is, away from the head and the toe.

Table 1. Effect of cross-sectional spacing. Ice jam near Ste-Anne, April 12, 1991

Value of ΔL (m)	Water level prediction	Ice jam thickness prediction
NA (no interpolation)	Good	Plausible; t_J ~ 1.4 m
2000	Good	Plausible; t_J ~ 1.4 m
1000	Good	Plausible; t_J ~ 1.4 m
500	Good	Plausible; t_J ~ 1.4 m
300	Good	Plausible; t_J ~ 1.4 m
200	Fair	Implausible; t_J ~ 1.4 m
100	Fair	Implausible; t_J ~ 1.3 m
50	Poor	Implausible; t_J ~ 1.2 m
20	Poor	Implausible, t_J ~ 0.8 m

The word "plausible" is used in Table 1 to indicate thickness variations that are consistent with observed and theoretically-derived shapes (Beltaos, 1993, 2001; Beltaos and Burrell, 2010): a plausible variation is characterized by a relatively thick toe, thin head and a generally continuous thickening in the downstream direction. The jam may also contain a segment of nearly-constant thickness ("equilibrium" reach; Beltaos, 1995). The profile of Fig. 4 does not meet the plausibility criteria. It contains two unexpected "bulges" in jam thickness and associated "kinks" in the water level profile. [Such features are not evident in Fig. 2 or in a simulation of the same jam using the more rigorous RIVJAM model (Beltaos *et al*., 1996)]. The cause of the HR model behaviour at small ΔL values is not known at present, but could be related to the trial-and-error iterative method of solving the differential equations and to the non-prismatic geometry of natural streams. Be that as it may, users should be aware of this feature and not assume that finer XS spacing will necessarily improve, or at least not worsen, model results.

For subsequent ice jam data sets, and especially with the shorter jams, it was found that the spacing should not be so large as to be of the same order of magnitude as the length of the jam. Therefore, judicious XS interpolation was applied in each case to ensure that there were enough sections to capture the channel bathymetry (~ 10 or more within the jammed reach) but not so many as might result in implausible profiles. The results of the calibrations are summarized in Table 2. They generally differ from those of the initial calibration that was reported by Tang and Beltaos (2008), largely as a result of the extensive use of the interpolation tool. In the case of Petite Brook, it was not possible to obtain a satisfactory profile with any combination of φ and V_{max}. The input values indicated in Table 2 resulted in the profile shown in Fig. 5, which appears to exhibit a pronounced toe-like feature, or bulge, upstream of the actual toe location, where it also under-predicts the water level.

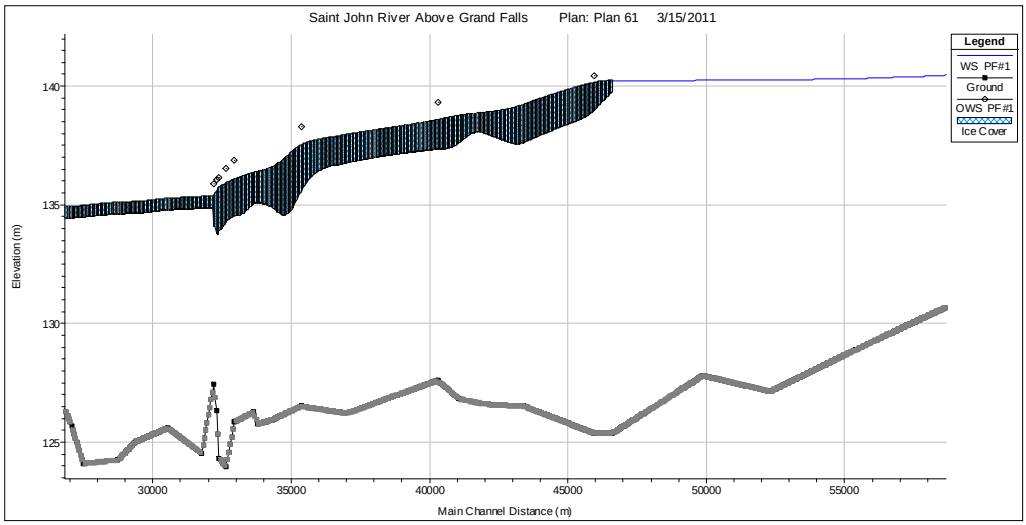

Figure 4. HEC-RAS graphical output for ΔL of 50 m (~ ¼ of channel width). Ice jam near Ste-Anne, 1991.

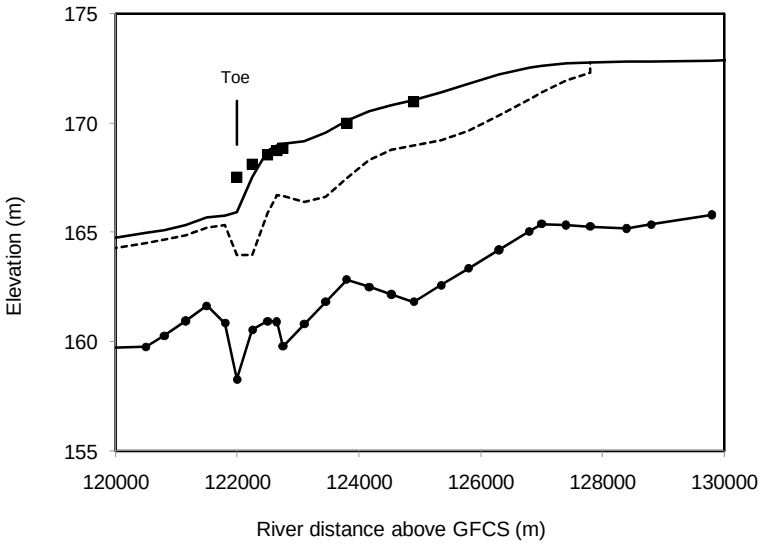

Figure 5. Ice jam near Petite Brook, April 21, 1996.

With the exception of the toe area, where the model suppresses the stability requirement, the calibration process indicated that good results can be obtained using a suitable set of input parameters. This set comprises mostly default values, but the internal friction angle φ ranges from 53° to 66°. This finding suggests that: (a) model calibration is necessary for good prediction; and (b) use of the default value for φ in upper St. John River would result in thicker jams and over-prediction of water levels. For practical purposes, Table 2 suggests that using a value of 55° for φ would be a largely conservative choice in the upper Saint John River reach, but less conservative than the default value.

An alternative calibration procedure was also tried, that is, fixing φ at 45° and changing V_{max}. This proved fruitless as it was not possible to obtain good agreement with the measurements. It was found further that relaxing the erosion constraint by selecting an arbitrarily high value (V_{max} = 10 m/s) did not seem to significantly affect the results of the present runs, in either calibration mode. Though not needed in the present calibrations, this result is particularly useful in cases of high river flows where the flow velocity under the sheet-ice cover approaches 1.5 m/s. In such

instances, HR generates highly implausible solutions that involve extremely long toe areas or merely extend the sheet-ice condition to the head of the jam. Where V_{max} is set at 10 m/s and the model computes velocities in excess of 1.5 m/s (unlikely to occur in nature), one may deduce that the toe of the jam is nearly grounded and most of the flow is taking place through the voids of the jam (Beltaos, 1993; 1999).

Table 2 Results of model calibration, Upper Saint John River

Ice jam location, Date	Jam length (km)	Calibration parameter		Value of ΔL (m)	Agreement of model output with measured water levels along the jam
		Internal friction angle	V_{max} (m/s)		
Near Ste-Anne de Madawaska, Apr. 12, 1991	13.8	56°	1.5 (default)	500	Very good; same for nearby jams in 1993 and 2009
Near St-Basile, Feb. 29 1996	4.2	66°	1.5	300	Good
Near Caron Brook, Feb. 27, 1996	1.1	60°	1.5	100	Fair
Near Ledges, April 11, 1993	0.6	61°	1.5	50	Good
Near Foley Brook, April 16, 1994	2.9	61°	1.5	300	Fair
Near Dickey April 16, 1994	5.9	61°	1.5	300	Fair (only one measured water level)
Near Petite Brook, April 21, 1996	6.3	53°	1.5	500	Fair

OPERATIONAL APPLICATION OF THE MODEL

Like other ice jam models, HR does not predict the location of an ice jam, which has to be specified by the user. Its main utility in operational forecasting mode is to examine the flooding potential of probable scenarios over the next few days. Typically, flow is predicted by means of a hydrological model that takes into account basin characteristics and uses weather forecasts and channel hydraulics to generate runoff and route it down the river. Different scenarios of probable ice conditions can be formulated by the forecaster based on his/her experience with the river and reach of interest. On occasion, this experience is augmented by the reports of local observers who carry out regular reconnaissance trips, as for example is done in New Brunswick.

After the record flood of 2008 in the Upper Saint John River, an attempt was made in 2009 to provide the communities above Grand Falls with detailed water level information and forecasts, as shown in Table 3. On April 6, a 12 km ice jam formed 26 km downstream of Edmundston. Using the river flows that were forecast by the SSARR model, the HR model was applied to determine ice-jam generated water levels for the next 3 days. The forecast for April 8 indicated that Edmundston water levels would reach 140.4 m, which exceeds the flood level. The actual measurement on April 8 indicated a value of 140.1 m. The jam advanced downstream and shortened during the next few days, but its location was tracked by the local observer. The HR

model was updated accordingly before issuing each subsequent 3-day forecast, and again found to give good results.

Table 3 Excerpt from 3-day water level forecast issued by Flow Forecast Center on April 7, 2009. All levels are expressed in metres above mean sea level.

Location	2008 W/L	Flood level	Actual	River forecast		
			0700 h	0700 h	0700 h	0700 h
			7-Apr	8-Apr	9-Apr	10-Apr
Baker Brook	151.4	150.8	147.75	148.2	148.4	148.0
Saint Hilaire	148.1	145.2	143.47	144.1	144.3	143.8
Edmundston	143.1	139.0	139.38	140.4	141.4	140.2
Sainte-Anne	138.8	138.3	134.61	135.4	136.1	135.6
Weather	Precip (mm)		3-16	5-26	0-2	0
(model input)	Temp (°c)		7/0	8/0	4/-2	5/-3

REMOTE MONITORING OF ICE BREAKUP DYNAMICS

The release of an ice jam generates a sharp wave, or jave, which propagates rapidly and causes precipitous increases in water velocities and levels as it passes by. The overall increase in water level is less than that caused by the "parent" jam, but it may be sufficient to flood low-lying areas next to the river. Moreover, the large water speed enhances erosive capacity and amplifies the momentum of moving ice blocks and slabs, imperiling homes and infrastructure, and potentially degrading aquatic habitat. Progress in the prediction of the hydraulic characteristics of javes (e.g. She and Hicks, 2006; Nolin *et al*., 2009) hinges on availability of good data sets.

As noted by Beltaos *et al*. (2011), the records of hydrometric gauges are spatially too sparse and temporally too coarse to capture the dynamics of javes. As an alternative, a remote measurement technique has been developed, which relies on portable pressure loggers, placed at selected locations along a study reach. The loggers are deployed shortly after hinge cracks develop in the ice cover and retrieved several weeks or months later, thus capturing breakup events as well as any subsequent open-water waves. Portability, ease of deployment, and sturdy housing are the main advantages of this technique, which is described in detail by Beltaos *et al*. (2011). The "sampling" interval, which can be as low as 1 second or even less, is also an attractive feature that not only enables capture of the sharpest javes but also helps in detecting instances where the logger may have been moved by ice.

Following a successful trial in 2007, eight loggers were deployed at various locations along the study reach in early April of 2009. The ensuing breakup event was accompanied by sizeable ice jams and javes, resulting in moderate flooding at and downstream of Edmundston (Fig. 1). Logger output is illustrated for a site near Baker Brook in Fig. 6, where it is seen to have captured not only the breakup rise, but also an open-water wave that occurred later in April. Though the first runoff event generated smaller flows than the second, ice jamming on April 5 caused much higher water levels. The "flat" segment in the water level record of Fig. 6 merely indicates that the actual water level was lower than the transducer.

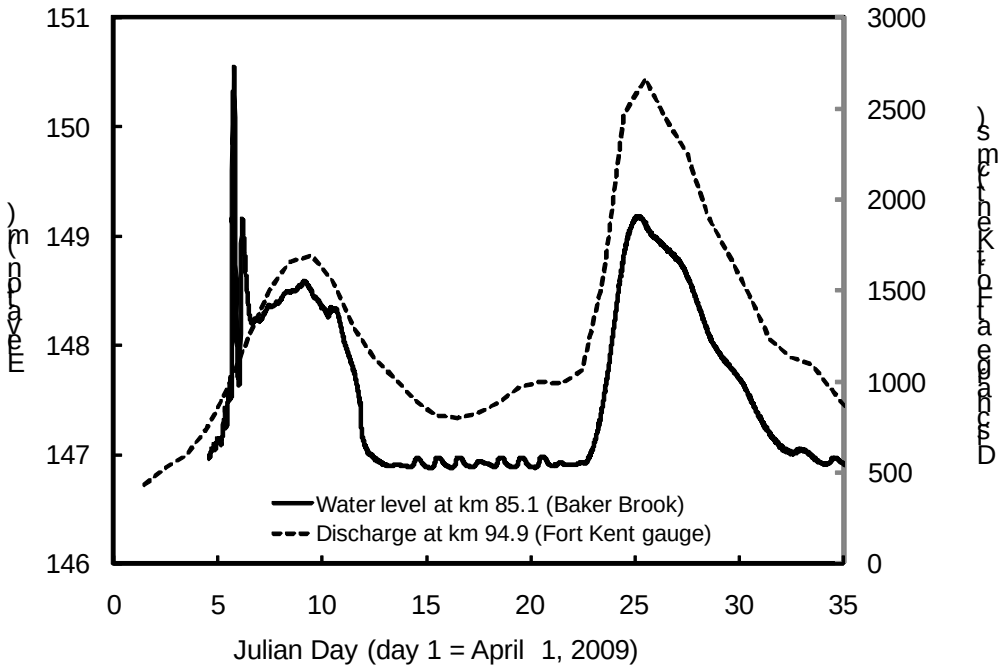

Figure 6. Water level variation near Baker Brook during April and early May 2009 as obtained from pressure logger output. Discharge is indicated on the secondary axis.

Details of breakup occurrences are illustrated in the larger-scale plots of Figs. 7 to 9. The very short record at km 91.6 (Fig. 8) reflects the relatively high-elevation placement of the logger, owing to prior formation of a minor jam slightly downstream. Even so, this record pinpoints the time of the release of this jam (sharp drop in water level), which triggered a small jave and dislodgment of the downstream ice cover. This movement culminated in the formation of a sizeable jam below Baker Brook, as reflected in the large rise at km 85.1 on April 5 (Fig. 8). This jam released shortly afterwards, generating the first jave captured at km 73.8 (Fig. 8).

At km 121, the water level was affected by a jam that had formed ~ 7 km downstream, and was subjected to several fluctuations before the final release at about midnight of April 5. The relatively small amplitude and large duration of the final jave in the 121 km record suggests that it was generated very far upstream. It is probable that this small jave contributed to the dislodgement of the downstream jam (toe at ~114 km), because a sharp jave arrived at km 103.1 very early on April 6 and was subsequently recorded at downstream sites, as far as km 54.6 (Figs. 8-10). The resulting large ice run was arrested in the flat reach downstream of Edmundston, causing a major jam. Over the next several days, this jam advanced by intermittent movements, which are reflected in the small javes of the downstream logger records of Fig. 9, where a gradual release is also indicated during April 12. Flooding of low-lying areas in Edmundston and of the old Trans-Canada Highway farther downstream occurred during April 7 and 8, but flood levels receded as the initial jam moved out (stage drop at km 54.6 and jave passing by kms 30.8 and 23.9; Fig. 9)

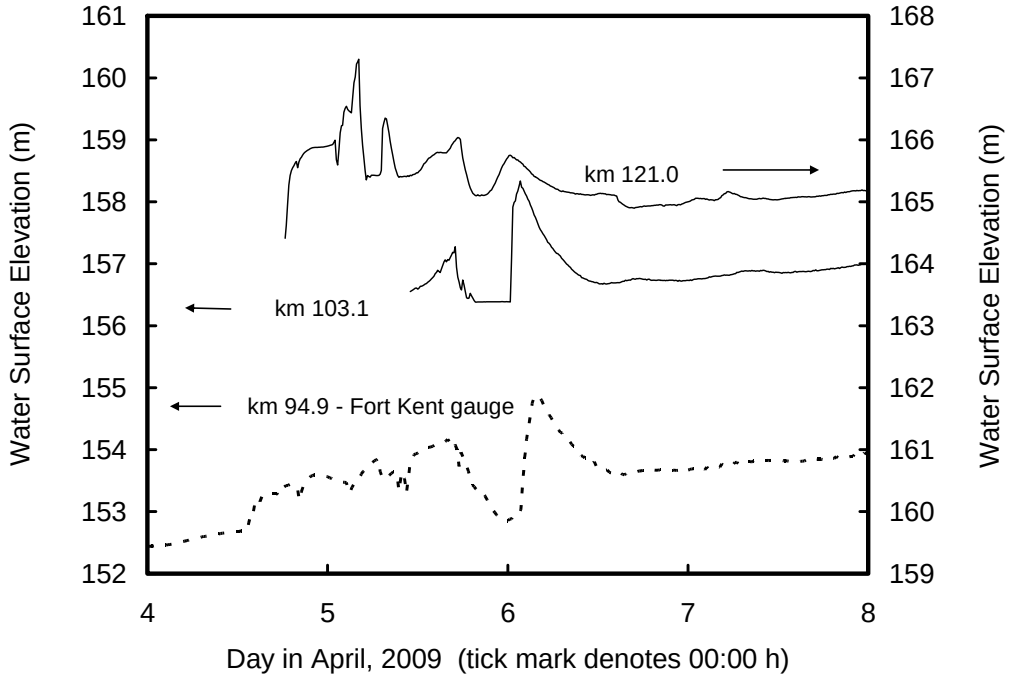

Figure 7. 2009 water level records in upper portion of study reach, St. Francis River confluence to Fort Kent-Clair. From Beltaos *et al*. (2011).

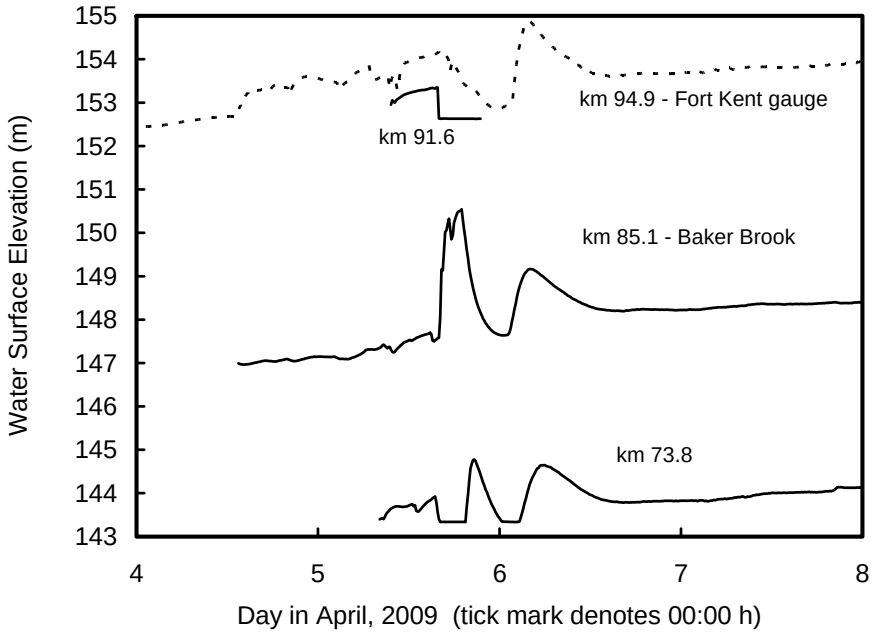

Figure 8. 2009 water level records in middle portion of study reach, Fort Kent/Clair to ~ 11 km above Edmundston. The loggers at 91.6 and 73.8 kms were respectively located near the small communities of Caron Brook and St-Hilaire. From Beltaos *et al*. (2011).

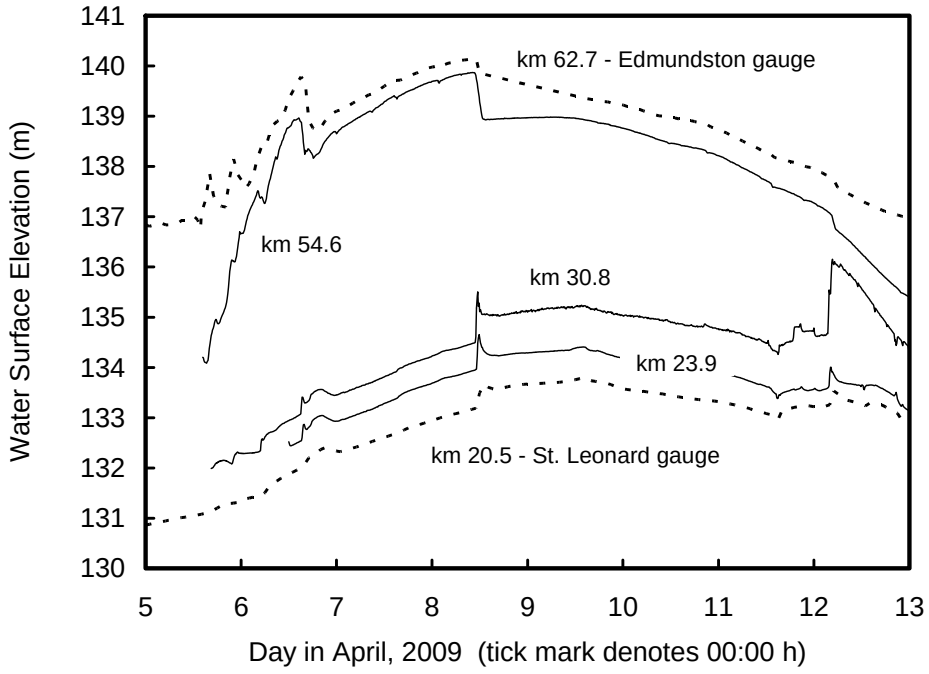

Figure 9. 2009 water level records in lower portion of study reach, Edmundston to St. Leonard. The loggers at 54.6 and 30.8 kms were respectively located near the small communities of St-Basile and Ste-Anne-de-Madawaska. The logger at km 23.9 was located slightly downstream of the mouth of Grande River. From Beltaos *et al*. (2011).

HYDRODYNAMIC PROPERTIES OF RECORDED JAVES

The hydrodynamic properties of a jave are quantified by such parameters as celerity, water velocity, discharge, and bed/ice cover shear stress. All these quantities change with time and distance from the point of release. The celerities of key wave features, such as the leading edge and the crest, cannot be measured at any particular location but average values can be determined between sites where the water level variations have been measured. Discharge and shear stress are derivative quantities, which could be determined if water velocity were known. Measurement of the latter, however, is hampered by the presence of moving ice. As an alternative, Beltaos and Burrell (2005) proposed an analytical method that examines the one-dimensional equations of motion of river flow within the rising limb of the jave, during which the hydrodynamic forces are largest.

The rising limb analysis method (RLAM) was applied to the waveforms recorded by the loggers, and hydrodynamic characteristics were calculated as outlined by Beltaos *et al*. (2011). Jave celerity decreased with distance traveled, but the leading edge always traveled faster than the crest, as can be seen in Fig. 10. In agreement with theoretical considerations (Beltaos, 2005), the leading edge celerity was no more than the corresponding celerity (C_g) of a gravity wave, which is approximately given by:

$$C_g \approx U_o + \sqrt{gh_o} \quad (1)$$

in which g = gravitational acceleration; and U_o, h_o = pre-jave average flow velocity and depth, respectively. Values of C_g ranged from 6 to 9 m/s, being highest in the relatively deep reach between Ste-Anne and St. Leonard.

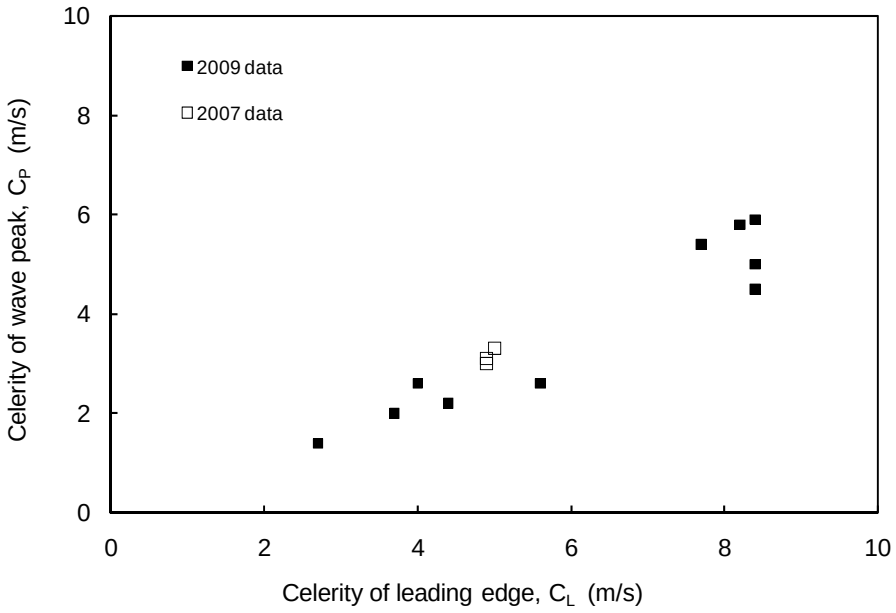

Figure 10. Celerity of jave peak (C_P) plotted versus that of the leading edge (C_L) for the 2009 breakup event. Note approximate relationship and ranges of respective values.

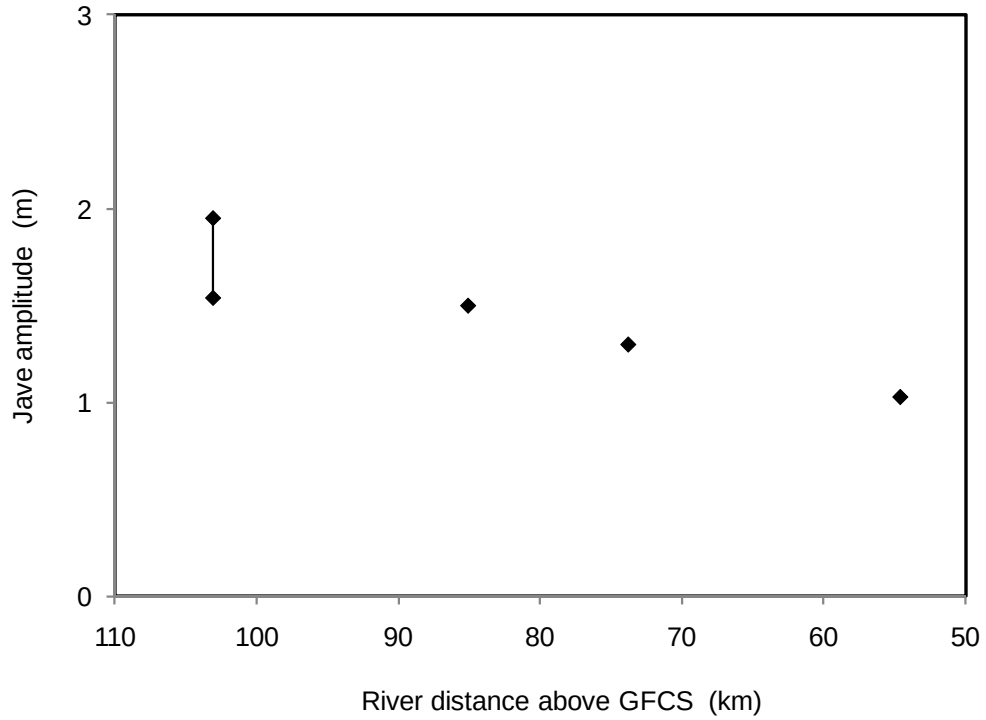

Figure 11. Attenuation of jave amplitude, April 6, 2009. The peak stage at km 103.1 may have been enhanced by downstream jamming; the jave amplitude can only be determined to within the indicated range.

Jave attenuation is illustrated in Fig. 11 for the wave of April 6 (Figs. 7-9), which propagated in open water within the depicted reach. The data points suggest an average attenuation rate of ~15 cm for each 10 km of travel. Downstream of km 54.6, the jave traveled under still-intact ice cover

and appears to have attenuated at an increased rate because the three subsequent measuring stations only registered a small disturbance (Fig. 9).

Actual water speeds were, as expected, lower than corresponding celerities, but often attained values of over 2 m/s. The discharge amplification factor (ratio of maximum during jave to pre-jave value) ranged from 1.3 to 2.6, and often exceeded 2. Bed shear stress exhibited the highest amplification factors (1.5 to 3.4), attaining values as high as 40 Pa., whereas pre-jave values were in the range 2 to 14 Pa. By comparison, the shear stress required to mobilize the "average" bed particle (size ~ 5 mm; Beltaos *et al*., 2011) is 4 Pa, according to the well known Shields criterion (Yalin, 1977). Therefore, large scale bed mobilization is very likely to occur during ice breakup events that result in sizeable ice jams. Though the erodibility of the river banks has not been quantified, it is probable that the large shear stress also leads to bank erosion. Moreover, these findings are consistent with the large increase of sediment concentration that is observed during breakup and the sharp spikes associated with javes (Beltaos and Burrell, 1999, 2000).

PROPERTIES OF RUNOFF WAVES

Capture of the post-breakup open water waves by the pressure loggers enabled a comprehensive test of the unsteady-flow capability of the HR model. Using the aforementioned bed Manning coefficients for the entire study reach (Model Calibration section), good results were obtained at the measuring stations including the four hydrometric gauges. Examples are presented in Fig. 12. In general, predicted water levels are within 0.2 m of measured values; however, there is one instance with a 0.7 m discrepancy (km 73.8, near the peak of the wave). This finding suggests that it may be possible to refine the initial calibration for n_b, which was entirely based on data from the hydrometric gauges at Dickey, Clair/Fort Kent, Edmundston, and St. Leonard.

Though unsteady, the flow conditions are hardly dynamic relative to javes. For instance, the average rate of rise along the rising limb of the runoff waves is in the neighbourhood of 0.06 cm/min, much less than corresponding jave values of ~ 6 cm/min (Beltaos *et al*., 2011). The subdued rate of rise makes it difficult to determine the celerity of the leading edge, which is not as well defined as in the case of javes. The celerity of the crest is more easily obtained by plotting distance versus the better defined time of crest (Fig. 13), fitting a polynomial trendline, and taking the derivative of the indicated function. This operation showed that the crest celerity, C_P, decreased from ~1.5 m/s at the upper end of the reach (km 144.5) to 1.3 m/s at km 95 and to 1.0 m/s at km 35. As might have been expected, this range is considerably lower than that of javes (Fig. 10).

Bed shear stress for open-water flow can be determined according to the relationship:

$$\tau_b = \rho g h \left(\frac{n_b V}{h^{2/3}} \right)^2 \quad (2)$$

in which ρ = freshwater density (1000 kg/m^3); h = average flow depth, assumed to be practically equal to the hydraulic radius of the flow; and V = average flow velocity; the bracketed term can be recognized as an equivalent expression to the friction slope, S_f. From available bathymetric data at the various measuring stations, flow area and average depth can be determined for any given water level. Using also model-generated discharge hydrographs, it is possible to determine V and thence τ_b. This operation resulted in maximum bed shear values ranging from 4.4 to 26.6 Pa. The lower end of the range describes the downstream stations (kms 23.9 and 30.8), where the water surface slope is severely reduced by the backwater of the GFCS. The upper end of the range applies to the upper segment of the study reach, between St Hilaire and Ledges (Fig. 1). An intermediate value (~ 15 Pa) was obtained for the 121.0 km station.

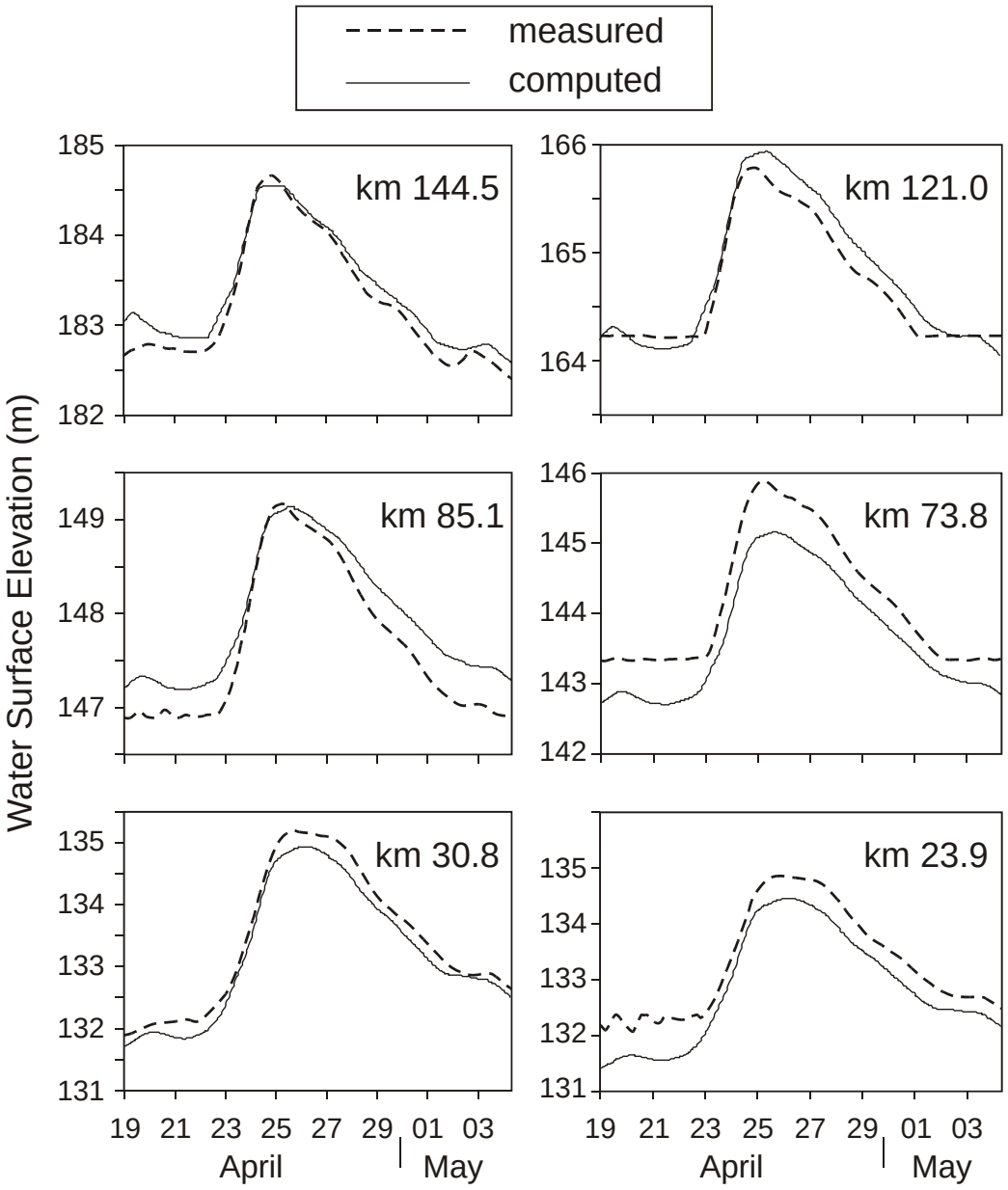

Figure 12. Examples of numerical simulations of runoff waves using the unsteady flow option of HR.

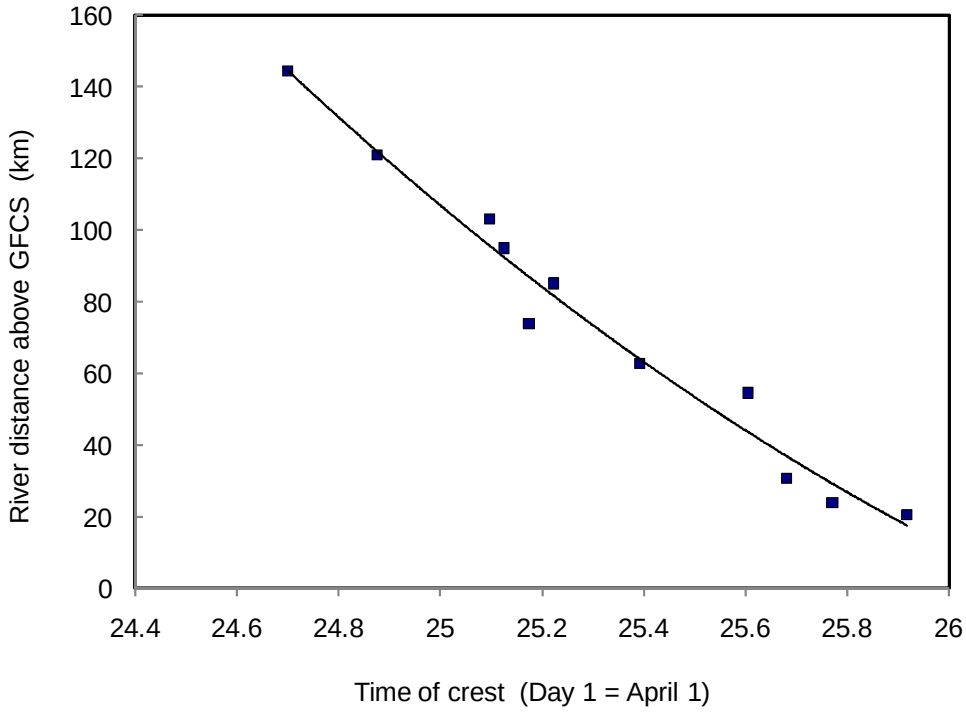

Figure 13. Plot of river distance versus the time of crest along with a polynomial fit to the data points. The slope of the line represents crest celerity in km/day.

The properties of the runoff waves are compared to those of javes in Table 4. The latter type is obviously much more dynamic than the former and can generate higher bed shear. It can also generate flow amplification factors that are comparable to those of runoff waves, which is rather remarkable given that the incoming (far upstream) river flow changes little during javes. Like javes, runoff waves are capable of mobilizing the bed of the river. Though transport rates would be smaller, runoff waves last much longer than javes (days as opposed to hours) and therefore can move greater volumes of bed material.

Table 4 Comparing hydrodynamic properties of ice- and runoff-generated river waves

Variable and units	Wave type	
	Jave[(1)]	Runoff
Celerity of leading edge (m/s)	2.7 to 8.4	Insufficient data
Celerity of crest (m/s)	1.4 to 5.9	1.0 to 1.5
Average rate of rise (cm/min)	0.3 to 12.0	0.04 to 0.09
Discharge amplification factor	1.4 to 2.6	2.6 to 2.9[(2)]
Peak bed shear stress (Pa)	4.2 to 40.9	4.4 to 26.6[(2)]

[(1)] Data from Beltaos *et al*. (2011); [(2)] Based on modelled flows

DISCUSSION

Both static and dynamic aspects of ice breakup processes were examined in the preceding sections. It was shown that modelling of ice jam water levels for forecasting purposes can be accomplished via the user-friendly HR model, which is suitable for a variety of hydraulic applications and includes a routine for steady-state ice jam computations. Like all models, HR has to be calibrated for specific river reaches, a task that requires good bathymetric documentation and some field measurements of water levels during actual ice-jam levels. A good understanding of river ice processes is prerequisite.

The calibration process revealed several noteworthy features, and especially the dependency of the output on the spacing of the computational XSs. The interpolation tool allows the user to generate plausible XSs between surveyed ones, but decreasing spacing eventually leads to poor results. Optimal spacing is likely to differ from case study to case study; the present experience suggests that the user should aim for at least 10 XSs within the length of an ice jam, but no more than ~30. It is not known whether these numbers apply to other rivers. It is recommended that model users test and modify them as needed for their own applications, based on the plausibility of computed profiles, as elaborated earlier (see also Table 1).

The range of internal friction angles (53° to 66°) that resulted from the calibration process (Table 2) is not fully in accord with known physics of ice jam behaviour, which points to a value of 56° to 59° (Beltaos, 2010). As far as angles are concerned, the discrepancy does not seem to be excessive. However, it is the passive resistance coefficient, K_p [$= \tan^2(45+\varphi/2)$] that largely determines the internal strength of the rubble in the jam. This coefficient is highly sensitive to the value of φ: it varies from 8.9 to 22.1 for φ = 53° to 66°, whereas the physically sound value is between 10.7 and 13.0 (φ = 56° to 59°). An additional discrepancy relative to known physics of ice jams arises from the values of the product $K_1K_p\tan\varphi$, which is equal to the ratio of the frictional side resistance within the rubble to the average effective vertical stress that is generated by buoyancy. For breakup jams, this ratio is equal to $\mu/(1-p)$, with μ known to be a near-constant coefficient, averaging 1.2 (Pariset *et al*., 1966; Beltaos, 1983, 1995). With p = 0.4, the quantity $K_1K_p\tan\varphi$ should be equal to ~2.0; however, the model-implied values range from 3.9 to 16.4. This suggests that the model requires unrealistically high side resistance, pointing in turn to over-prediction of the driving forces that are applied on the jam. The over-prediction is very likely related to the shear stress that is exerted by the flow on the underside of the jam (τ_i), and calculated by assuming that the hydraulic resistance coefficient of the bed (n_b) is the same as in open water conditions. However, empirical and theoretical evidence (Beltaos, 2001; Alcoa 2004) suggest that the value of n_b increases considerably underneath an ice jam, owing to the extreme roughness of the upper boundary and the resulting modification of the flow structure.

Though the model can be made to "work" with suitable calibration, the above findings suggest limited transferability among different rivers or different reaches of the same river. This concern can be addressed with relatively simple revisions to the ice-jam equations used in HR, based on current understanding of internal strength and hydraulic roughness characteristics of ice jams (Beltaos, 2001, 2010).

At present there is very limited modelling capability for dynamic breakup events, such as javes and ice runs. The best way to understand their hydrodynamic properties and assess their erosion potential is by measurement. This is not an easy task, but it has been shown that waveforms can be captured in satisfactory detail using suitably placed portable loggers that are retrieved after the event. In turn, the measured waveforms can be processed using the RLAM method to quantify the amplification of such variables as velocity, discharge, and shear stress. The loggers can also be used for measurements of ordinary runoff waves, as was done during the 2009 field program. The timing of logger placement is a key factor, especially for the breakup event. If a logger is installed too early, a return of cold weather may cause it to freeze and become a part of the ice cover; if too late, its meaningful record would be limited by the relatively high elevation, as illustrated by the 91.6 km line in Fig. 8. As the timing of breakup depends on weather conditions, all necessary equipment should be ready to go well in advance and members of the field crew prepared to depart on short notice.

The overall satisfactory outcome of the modelling effort suggests that application can be extended to other ice-jam prone reaches of the Saint John River, such as the Perth-Andover area, which is located upstream of the Beachwood dam, and the Simonds – Hartland area downstream of this dam. Though not shown in Fig. 1, both areas are located in the middle Saint John reach. Bathymetric information is already available and there are a few case studies of past ice jams that can be used for model calibration. Similarly, the hydrodynamic properties of javes can be assessed using the portable probe methodology.

SUMMARY AND CONCLUSIONS

Ice jams cause major flooding and severe damages to communities and infrastructure along the Saint John River. There is a growing need to develop capability in forecasting and analyzing ice-jam-related flood events, and anticipating the potential for increased risks as a result of a changing climate. The ice routine of the HR model has been calibrated using previously documented ice jam events along the upper Saint John River. In the course of this work, certain model strengths and weaknesses were identified. On the positive side, HR provides a user-friendly and flexible framework where many types of hydraulic computations can be accommodated under open-water, sheet-ice and ice-jam conditions. The recently added XS interpolation tool significantly enhances the user's ability to improve output and obtain plausible ice jam profiles. The writers were surprised to find that reducing the spacing of XSs below a case-specific threshold results in deteriorating output. In general it is possible to obtain good results by judicious selection of this spacing and of the values of model parameters. The latter, however, do not conform to current understanding of ice jam physics, suggesting limited transferability. This limitation can be easily addressed in a future version of the model.

At present, dynamic aspects of breakup can best be assessed by measurement. It is shown that the portable logger technique can provide detailed data on the forms of various javes, which can be analyzed to quantify their hydrodynamic properties. The 2009 javes advanced as rapidly as 8.4 m/s with attenuation rates of ~ 15 cm per 10 km of travel in open water. Presence of an ice cover appears to enhance attenuation. Sharp bed shear stress amplification indicated potential for large-scale channel boundary mobilization. The portable loggers can record well past the breakup event to also capture the open-water, spring flood. This information is particularly useful in testing the performance of the unsteady-flow, open-water routine of HR (or of any other model) as a means of forecasting runoff-generated floods.

ACKNOWLEDGMENTS

The authors thank their respective agencies for funding this study and gratefully acknowledge technical support by Earl Walker (Ret.) and Charlie Talbot of Environment Canada. Ice observation notes by local observer Roy Gardner and unpublished hydrometric data provided by the WSC Fredericton office are appreciated.

REFERENCES

Alcoa. 2004. Addendum to the comprehensive characterization of the Lower Grasse River. Volume I – *Main Report, Grasse River Study Area, Massena, New York*.

Beltaos S. 1983. River ice jams: theory, case studies and applications. ASCE *Journal of Hydraulic Engineering* **109**: 1338-1359.

Beltaos, S. 1995. Chapter 4: Theory. In: *River Ice Jams* (S. Beltaos, ed.), Water Resources Publications, Highlands Ranch, Co., USA.

Beltaos S. 1993. Numerical computation of river ice jams. *Canadian Journal of Civil Engineering* **20**: 88–89.

Beltaos S. 2002. Effects of climate on mid-winter ice jams. *Hydrological Processes* **16**: 789−804.

Beltaos S. 2001. Hydraulic roughness of breakup ice jams. ASCE *Journal of Hydraulic Engineering* **127**: 650−656.

Beltaos S. 2004. Climate impacts on the ice regime of an Atlantic river. *Nordic Hydrology* **35**: 81−99

Beltaos S. 2005. Field measurements and analysis of waves generated by ice-jam releases. *Proceedings, 13th Workshop on the Hydraulics of Ice Covered Rivers, Hanover, NH, September 15-16, 2005, pp. 227-249.* Available in CD format. CGU-HS Committee on River Ice Processes and the Environment, Edmonton, Canada.

Beltaos S. 2008. Chapter 7: Ice jams. In: *River Ice Breakup* (S. Beltaos, ed.). Water Resources Publications, Highlands Ranch, Co., USA.

Beltaos S. 2010. Internal strength properties of river ice jams. *Cold Regions Science and Technology* **62**: 83–91.

Beltaos S, and Burrell BC. 1999. Transport of metals on sediment during the spring breakup of river ice. In: *Ice in Surface Waters* (Hung Tao Shen, ed.). In *Proceedings, 14th International Symposium on Ice, held at Potsdam, NY, 27−31 July 1998*, IAHR, A.A. Balkema, Rotterdam, Vol. 2, 793−800.

Beltaos S, and Burrell, BC. 2000. Suspended sediment concentrations in the Saint John River during ice breakup. In *Proceedings, 2000 Annual Conference of the Canadian Society for Civil Engineering, London, Ontario*, 235−242.

Beltaos S, and Burrell BC. 2005. Determining ice-jam surge characteristics from measured wave forms. *Canadian Journal of Civil Engineering* **32**: 687−698.

Beltaos S,and Burrell BC. 2010. Ice-jam model testing: Matapedia River case studies, 1994 and 1995. *Cold Regions Science and Technology* **60**: 29–39.

Beltaos S, and Wong J. 1986. Downstream transition of river ice jams. *ASCE Journal of Hydraulic Engineering* **112**: 91-110.

Beltaos S, Burrell BC, and Ismail S. 1996. 1991 Ice jamming along the Saint John River: a case study. *Canadian Journal of Civil Engineering* **23**: 381–394.

Beltaos S, Burrell BC, and Ismail S. 1994. Ice and sedimentation processes in the Saint John River, Canada. In *Proceedings of IAHR International Ice Symposium, Trondheim, Norway, August*, Vol. 1, 11−21.

Beltaos S, Ismail S, and Burrell BC. 2003. Mid-winter breakup and jamming on the upper Saint John River: a case study. *Canadian Journal of Civil Engineering* **30**: 77–88.

Beltaos S, Rowsell R, and Tang P. 2011. Remote data collection on ice breakup dynamics: Saint John River case study. *Cold Regions Science and Technology* **67**: 135−145.

Carson R, Beltaos S, Groenevelt J, Healy D, She Y, Malenchak J, Morris M, Saucet J-P, Kolerski T, and Shen HT. 2011. Comparative testing of numerical models of river ice jams. *Canadian Journal of Civil Engineering* **38**: 669−678.

Flato GM, and Gerard R. 1986. Calculation of ice jam profiles. In *Proceedings, 4th Workshop on River Ice, Montreal, Canada*, Paper C-3.

Hare FK, Dickison RB, and Ismail S. 1997a. Variation of climate and streamflow over the Saint John River Basin since 1872. In *Proceedings of 9th Workshop on River Ice, Fredericton, Canada*, 1−21.

Hare FK, Dickison RB, and Ismail S. 1997b. Climatic variation the Saint John River Basin: an examination of regional behaviour. Report CCD 97-02, *Climate Change Digest*, Environment Canada, Downsview, Canada.

Humes, TM, and Dublin, J. 1988. A comparison of the 1976 and the 1987 St. John River ice jam flooding with emphasis on antecedent conditions. In *Proceedings of Workshop on the Hydraulics of River Ice/Ice Jams, Winnipeg, Canada*, National Research Council of Canada Associate Committee on Hydrology, Ottawa, Canada, 43−62.

Jasek M, and Beltaos S. 2008. Chapter 8. Ice-jam release: javes, ice runs and breaking fronts. In: *River Ice Breakup*, (S. Beltaos ed.). Water Resources Publications, Highlands Ranch, Co., USA.

Nezhikhovskiy RA. 1964. Coefficients of roughness of bottom surface on slush-ice cover. *Soviet Hydrology*, Washington, Am. Geoph. Union, 127−150.

Nolin S, Roubtsova V, Morse B, and Quach T. 2009. Smoothed particle hydrodynamics hybrid model of ice-jam formation and release. *Canadian Journal of Civil Engineering* **36**: 1133–1143.

Pariset E, Hausser R, and Gagnon A. 1966. Formation of ice covers and ice jams in rivers. *ASCE Journal of the Hydraulics Division* **92**: 1−24.

She Y, and Hicks F. 2006. Modelling ice jam release waves with consideration for ice effects. *Cold Regions Science and Technology* **45**: 137−147.

Tang P, and Beltaos S. 2008. Modelling of river ice jams for flood forecasting in New Brunswick. In Proceedings, *65th Eastern Snow Conference, Fairlee, Vermont, USA* (R. Hellström and S. Frankenstein, eds). Bridgewater State College and ERDC-CRREL, 167−178.

Yalin MS. 1977. *Mechanics of sediment transport*. Pergamon Press, Toronto.

Reconstructing Snowmelt Runoff in the Yukon River Basin Using the SWEHydro Model and AMSR-E Observations

JOAN M. RAMAGE[1] AND KATHRYN A. SEMMENS[2]

ABSTRACT

Snowmelt timing and snow water equivalent (SWE) from the Advanced Microwave Scanning Radiometer for EOS (AMSR-E) are used as inputs to the SWEHydro model to simulate spring snowmelt runoff in high-latitude, snow-dominated drainages. AMSR-E data from 2003 to 2010 are used to determine the timing of melt onset and snow saturation based on changes in brightness temperature (Tb) and diurnal amplitude variations (DAV). Pre-melt SWE data are combined with terrain information and melt rate estimates to calculate runoff. After melt onset there is a "melt transition period" with daytime melt and nocturnal refreeze. The melt transition is characterized by high Tb oscillations (high DAV). At the end of high DAV (EHD), the snowpack is melting at a higher rate. The model uses four parameters: snowmelt rate during and after melt transition (defined by Tb and DAV thresholds), and flow timing during and after melt transition. The model effectively simulates spring freshet, peak timing and magnitude, and volume (between days 50-180) in basins lacking sufficient meteorological measurements for conventional models. We compare the model response in the Pelly and Stewart Rivers, tributaries to the Yukon River, to evaluate model parameters in broadly similar basins under varying conditions. Simulated freshet timing is strongly related to snowmelt timing, and the modeled hydrograph is most sensitive to the flow timing parameter. This observationally based model has potential as a module for quantifying spring snowmelt runoff and timing in physically based models.

Keywords: AMSR-E; SWEHydro; snowmelt runoff; Yukon, Pelly River, Stewart River

INTRODUCTION

Global warming is being felt most dramatically at high latitudes (e.g. ACIA, 2004; IPCC, 2007) through changes in snowpack, melt timing and patterns, permafrost coverage, and clouds, all of which determine the flux of fresh water from drainage basins. Ecosystems, biogeochemical cycles, the hydrological cycle, and ocean productivity are expected to respond to these global warming driven hydrologic changes (e.g. White *et al*., 2007). Studies of high latitude rivers show that both annual and seasonal discharges are changing due to both natural causes and human infrastructure such as dams. Snow distribution and melt timing correspond well with snowmelt runoff and are largely responsible for observed seasonal changes (Kane *et al*., 2000; White *et al*., 2007 and references therein).

This research uses Advanced Microwave Scanning Radiometer for EOS (AMSR-E) satellite observations of spatially distributed snow characteristics such as snow water equivalent (SWE)

[1] Lehigh University, Earth and Environmental Sciences Department, 1 West Packer Ave., Bethlehem, PA 18015-3001, ramage@lehigh.edu

[2] Lehigh University, Earth and Environmental Sciences Department, 1 West Packer Ave., Bethlehem, PA 18015-3001, kas409@lehigh.edu